

# Structural influence on charge-carrier lifetimes in TiO<sub>2</sub> powders studied by microwave absorption

C. COLBEAU-JUSTIN\*, M. KUNST

*Hahn-Meitner-Institut, Abteilung Solare Energetik, Glienicke Straße 100,  
D-14109 Berlin, Germany*

D. HUGUENIN

*Rhodia, Centre de Recherche d'Aubervilliers, 52 rue de la Haie-Coq,  
F-93308 Aubervilliers Cedex, France  
E-mail: colbeau@limhp.univ-paris13.fr*

A set-up for contactless transient photoconductivity measurements on powders by the Time Resolved Microwave Photoconductivity (TRMC) method has been realized. These measurements have been used as a tool for the investigation of excess charge-carrier lifetimes in TiO<sub>2</sub> (anatase and rutile) powders. The influence of laser wavelength and intensity on TRMC decay shows the importance of the fast-recombination processes. The presence of a long time tail in the TRMC signals of the anatase modification of TiO<sub>2</sub> is attributed to quenching of this recombination by hole-trapping at the surface. The influence of surface treatment by ethanol and water on TRMC decay evidences that dominant effects are bulk recombination in rutile and surface trapping in anatase. The influence of doping in rutile shows that increasing the doping rate accelerates the decay whatever the doping type is. The doping element acts as an impurity favoring recombination by creation of structural defects. The influence of thermal treatment in anatase shows that increasing the thermal treatment temperature increases the lifetimes. High crystalline quality leads to long charge-carrier lifetimes. The results are discussed in view of their relevance for photocatalysis. © 2003 Kluwer Academic Publishers

## 1. Introduction

The last decades, TiO<sub>2</sub> has replaced other materials used as white pigments in coatings, plastics and inks [1]. The interest of TiO<sub>2</sub> is linked to several advantages, especially its refractive index which is the highest of the white stable compounds and its adjustable particle size. These two points allow obtaining a pigment with the best hiding power of all white pigments. Furthermore, it is a non-toxic, quite stable and cheap product.

In 1972, Fujishima and Honda [2] have described the TiO<sub>2</sub>-catalyzed photolysis of water. The photocatalytic activity was considered at first as harmful, because it was the cause of the degradation of the polymeric matrix in which TiO<sub>2</sub> was incorporated. So, the first studies dealing on with this activity were to obtain its inhibition.

Afterwards, it was shown that it was possible to use the activity in environmental applications, like photodegradation of organic pollutants in water and in air [3–7]. The aim of these studies was the characterization of the photocatalytic activity of commercial powders.

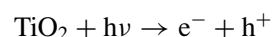
While water and air purification is a high-competition technique field, the self-cleaning of TiO<sub>2</sub> covered

surface appears to open possibilities which cannot be provided by other technologies [8, 9]. The most significant initiatives are realized in Japan where some companies are selling bacteria-killing and sterilizing TiO<sub>2</sub>-covered tiles, sets of tunnels lights which avoid their covering by carbon and oil layers, filters to catch cigarette smoke, antifog mirrors and glasses.

Some reviews [10–15] present recent developments in theoretical and applied photocatalysis.

TiO<sub>2</sub> is a semiconductor that crystallizes in two polymorphic forms: rutile and anatase. The bandgaps of anatase and rutile are respectively 3.23 eV and 3.1 eV. Anatase is a metastable form that transforms to rutile at high temperature.

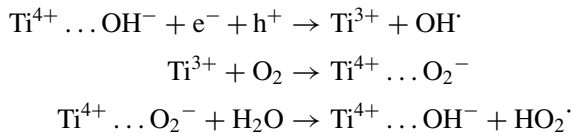
Under UV light illumination, the photon energy is higher than the bandgap and the creation of an electron-hole pair occurs:



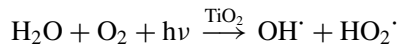
If the charge-carriers do not recombine, the titanium or the oxygen ions can trap them. In this case, TiO<sub>2</sub> shows a photocatalytic activity in presence of O<sub>2</sub> and

\*Present address (for correspondence): Laboratoire d'Ingénierie des Matériaux et des Hautes Pressions, CNRS-UPR 1311, Université Paris 13, 99 avenue J. B. Clément, 93430 Villetaneuse, France

H<sub>2</sub>O, which is described by the following mechanism [4]:



So the global reaction is:



This shows that the photocatalytic activity leads to the formation of free radicals, which are causing degradation of organic compounds. The reaction with a polymer can be written:



The photocatalytic activity is therefore linked to excess charge carrier dynamics, i.e., the creation and the temporal evolution of excess charge-carriers in the semiconductor. Whatever the application of TiO<sub>2</sub> is, pigment or photocatalyst, it is necessary to understand the mechanisms leading the activity in order to control it and to supply the specific product for the application.

The first aim of this work was to understand the relation between charge-carrier lifetimes and material structural parameters. A contactless transient photoconductivity method, the *Time Resolved Microwave Conductivity* (TRMC) method, has been chosen as a tool for the investigation of the charge-carrier lifetimes in TiO<sub>2</sub> materials.

Previous works, concerning charge carrier dynamics in powders using microwave photoconductivity or other techniques like laser flash photolysis, microwave photodielectric response, have been reported on MgO and Al<sub>2</sub>O<sub>3</sub> [16], MoS<sub>2</sub> and MoSe<sub>2</sub> [17], ZnO [18] and TiO<sub>2</sub> [16, 19–24]. These works present results on analyses techniques and charge-carrier dynamics (kinetic constants, recombination rates, mechanisms. . .) on various compounds but show a lack of information concerning relation between material structural parameters (structure, microstructure, crystalline quality, particle size, doping level, surface state. . .) and charge carriers lifetimes.

In this work, a sample holder has been especially designed to perform TRMC measurements on various TiO<sub>2</sub> powder samples. TRMC measurements have been realized on anatase and rutile powders to confirm the previously observed [24] differences between the two modifications. Experiments as function of laser intensity and wavelength have been carried out in order to understand dominant phenomena (recombination or trapping) concerning charge-carrier dynamics after the laser pulse.

The importance of surface phenomena has been studied on both modifications realizing simple surface treatments with water and ethanol. The influence of structural parameters has been studied by following the effect of the doping on rutile and the thermal treatment temperature on anatase.

The last aim of this work was to know if a correlation between TRMC measurements and material photocatalytic activity is possible.

## 2. TRMC principle

The TRMC [25–27] method is based on the measurement of the change of the microwave power reflected by a sample induced by laser pulsed illumination of this sample. The relative change, ( $\Delta P(t)/P$ ) of the reflected microwave power is caused by a variation  $\Delta\sigma(t)$  of the sample conductivity induced by the laser. For small perturbations of conductivity, a proportionality between  $\Delta P(t)/P$  and  $\Delta\sigma(t)$  has been established [25]:

$$\frac{\Delta P(t)}{P} = A\Delta\sigma(t) = Ae \sum_i \Delta n_i(t)\mu_i \quad (1)$$

$\Delta n_i(t)$  is the number of excess charge-carriers  $i$  at time  $t$ ,  $\mu_i$  is the mobility of charge carrier  $i$ . The sensitivity factor  $A$  is independent of time, but dependent on the microwave frequency and on the conductivity of sample.

For the present work, the Equation 1 can be reduced to mobile electrons in the conduction band and holes in the valence band. Trapped species can be neglected because of their small mobility.

$$\frac{\Delta P(t)}{P} = A\Delta\sigma(t) = Ae(\Delta n(t)\mu_n + \Delta p(t)\mu_h) \quad (2)$$

$\Delta n(t)$  is the number of excess electrons,  $\mu_n$  is the mobility of electrons,  $\Delta p(t)$  and  $\mu_h$  are the corresponding properties of holes.

The TRMC signal ( $\Delta P(t)/P$  or  $I(t)$ ) obtained by this technique is called (microwave) photoconductivity, it allows to follow directly, on the 10<sup>-9</sup>–10<sup>-3</sup> s time scale, the decay of the number of electrons and of the holes after the laser pulse by recombination or trapping of the charge-carriers.

In the specific case of TiO<sub>2</sub>, the TRMC signal can be attributed to the electrons because their mobility is much larger than the hole's one [28]. So the kinetics of holes is observed only indirectly, by their influence on electron kinetics.

The TRMC signal can be characterized by two parameters: the maximum value ( $I_{\text{max}}$ ) and the decay  $I(t)$ .  $I_{\text{max}}$  is determined by the electron mobility and by fast decay processes with an appreciable activity during the excitation (i.e., the first 10 ns). These two contributions cannot be separated easily for a system as TiO<sub>2</sub> powder. In general, a high value of  $I_{\text{max}}$  can be considered as reflecting good electronic properties due to good crystalline structure of the sample. Because the signal decay is not purely exponential, the general decay shape is characterized by several half-time lives,  $\tau_{1/2}$  is the time to obtain intensity  $I_{\text{max}}/2$  of the signal,  $2\tau_{1/2}$  to obtain  $I_{\text{max}}/4$ . As important phenomena occur at the beginning of the pulse, it is more convenient to characterize the decay with the  $I_{40\text{ns}}$  value, which is the intensity of the signal 40 ns after the beginning of the pulse. The ratio  $I_{40\text{ns}}/I_{\text{max}}$  is also reported.

## 3. Experimental set-up

The principle of the measurements is to place the powder sample inside a wave-guide, to proceed to its

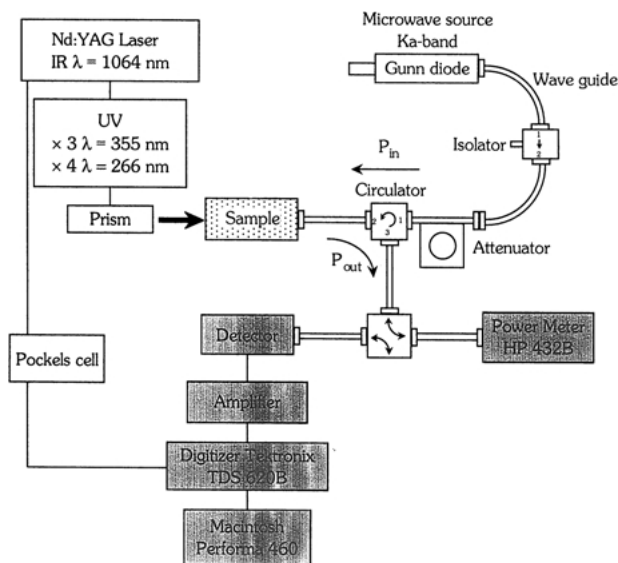


Figure 1 TRMC experimental set-up.

illumination by a UV pulsed laser, and then to follow the temporal evolution of microwave power reflected by the sample. The experimental set-up is displayed in Fig. 1 and shows four sections: the microwave circuit (white), the detection and signal treatment (dark gray), the UV source (light gray), the sample (stippled).

The incident microwaves are generated by a Gunn diode in the Ka band (28–38 GHz). The experiments were carried out at 31.4 GHz, this frequency corresponds to the highest microwave power. The reflected microwaves are detected by an Schottky diode. The signal is amplified and displayed on the digitizer.

Pulsed light source is an Nd:YAG laser giving an IR radiation at  $\lambda = 1064$  nm with a 10 Hz frequency. Full width at half-maximum of one pulse is 10 ns. UV light is obtained by tripling (355 nm) or quadrupling (266 nm) the IR radiation. The maximum light energy density received by the sample is  $1.3 \text{ mJ} \cdot \text{cm}^{-2}$  for both wavelengths.

A polymeric sample holder has been specifically designed for powder measurements. It is represented in

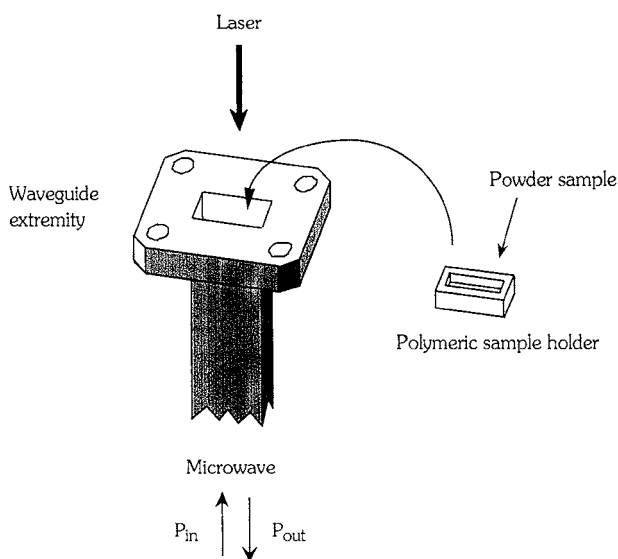


Figure 2 Sample holder design.

Fig. 2. With this design, the sample can be illuminated in powder form, inside the wave-guide. This allows the best microwave response.

The apparent periodic structure in some decay profiles is due to high sinusoidal noise created by interference between the microwave detector and the laser power generator.

## 4. Results on $\text{TiO}_2$ powders

### 4.1. Influence of the laser wavelength on the TRMC signal

The TRMC signals obtained on rutile are characterized by a very fast decay that is independent of the excitation wavelength (266 nm or 355 nm). Anatase powders show another behavior. The TRMC signals, recorded at 266 and 355 nm on B3 anatase powder, are represented on Fig. 3 (the  $I_{\text{max}}$  values are normalized to facilitate the decay comparison). The inset shows the decay for 355 nm for a longer time range (0–10  $\mu\text{s}$ ). The figure shows a slower decay over the 10–40 ns range after the beginning of the pulse for 355 nm than 266 nm. After 40 ns, the decay becomes identical for both wavelengths. This can be explained by the fact that the absorption coefficient of  $\text{TiO}_2$  is larger at 266 nm than at 355 nm. This means that the penetration length is lower at 266 nm light which makes the excess charge carrier concentration for 266 nm excitation larger than for 355 nm excitation at the same excitation density. As general feature, the electron-hole recombination rate becomes faster with higher carrier concentration, the decay is faster after 266 nm excitation than after 355 nm excitation. This point shows the important role played by the electron-hole recombination at the beginning of the decay, especially for 266 nm excitation. This point will be also discussed in the section 4.3.

### 4.2. Differences between rutile and anatase

The TRMC signals measured on B3 anatase and R1 rutile, are displayed in Fig. 4 (the  $I_{\text{max}}$  values are normalized).  $I_{\text{max}}$ ,  $I_{40\text{ns}}$  and  $\tau_{1/2}$  values for various rutile and anatase samples are collected in Tables I and II. It appears as a general behavior that rutile samples show faster decay than anatase samples. In anatase powders, the TRMC signal decays over an extended time range from nanoseconds to milliseconds. In the rutile powder a rather small TRMC signal is observed after 40 ns. This difference, previously observed by Schindler *et al.* [24], was interpreted in the following way: the short free electron lifetime in rutile is due to a high recombination rate whereas in anatase there is a competition between a fast recombination process and a fast trapping of a part of charge-carriers which are not participating to the TRMC signal (i.e., the holes). This trapping process reduces the number of holes available for recombination processes and so increases the lifetime of charge-carriers that are contributing to the TRMC signal (the electrons). If an appreciable part of the excess holes are trapped, the decay of the excess electrons is controlled by the relaxation (emission) time of trapped holes. This explanation implies the existence of an appreciable

TABLE I References, structural parameters and TRMC results on rutile samples ( $\lambda = 355$  nm)

Reference	Nature	Analysis	$I_{\max}$ (mV)	$I_{40\text{ns}}$ (mV)	$I_{40\text{ns}}/I_{\max}$ (%)	$\tau_{1/2}$ (ns)	$2\tau_{1/2}$ (ns)	$3\tau_{1/2}$ (ns)
Rutile R1	Cr doping	Nb = 830 ppm, Cr = 0.90 ppm	4.3	0.5	12	15	20	32
Rutile R2	Cr doping	Nb = 830 ppm, Cr = 1.15 ppm	4.2	0.3	7.1	12	18	25
Rutile R3	Cr doping	Nb = 830 ppm, Cr = 1.80 ppm	4.9	0.3	6.1	12	18	25
Rutile R4	Cr doping	Nb = 830 ppm, Cr = 2.25 ppm	4.2	0.2	4.8	12	15	18
Rutile S1	Nb doping	Nb = 1753 ppm, Cr = 0.89 ppm	4.2	0.4	9.5	14	18	25
Rutile S2	Nb doping	Nb = 2343 ppm, Cr = 0.90 ppm	5.0	0.2	4.0	12	16	22

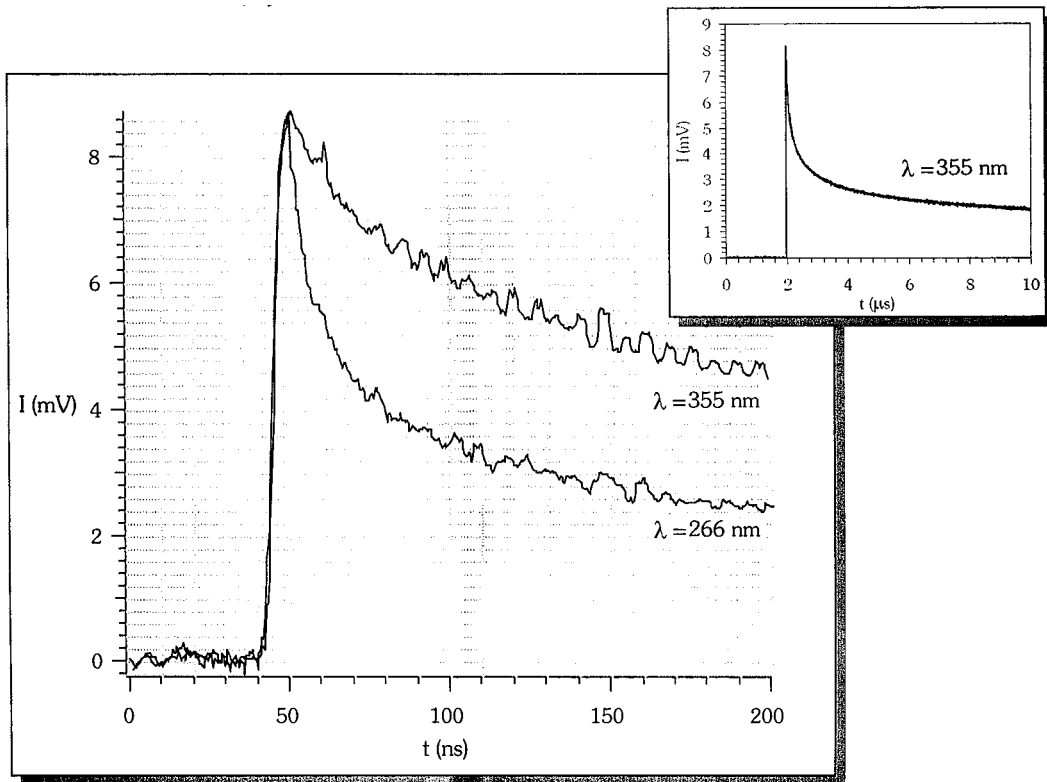


Figure 3 Influence of the laser wavelength on the TRMC signal of anatase—Inset:TRMC decay in a large time range (0–10  $\mu\text{s}$ ) for  $\lambda = 355$  nm.

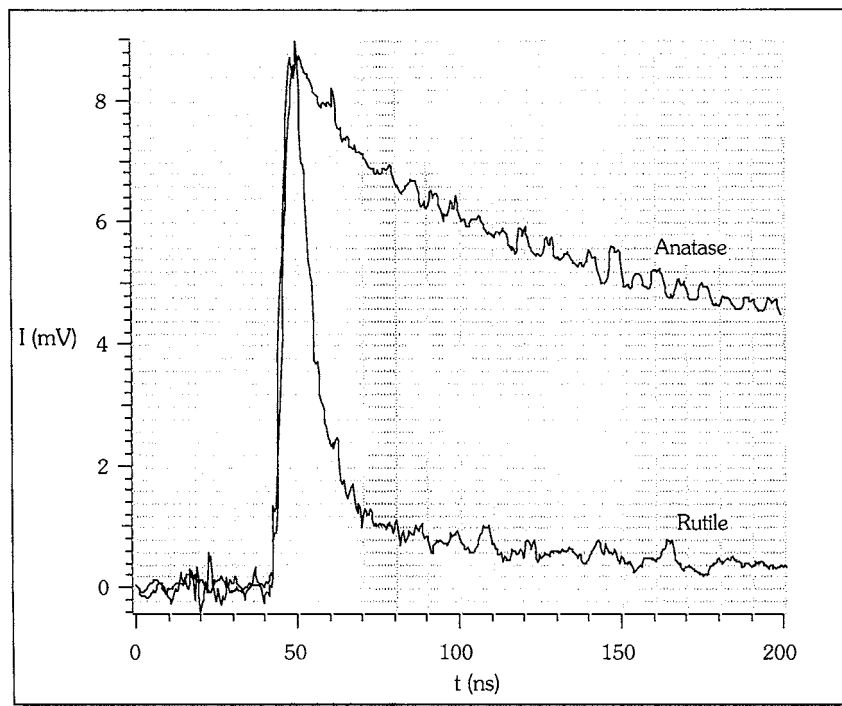


Figure 4 Differences between rutile and anatase on the TRMC signal.

TABLE II References, structural parameters and TRMC results on anatase samples ( $\lambda = 355$  nm)

Reference	Thermal treatment (°C)	BET surface area (m <sup>2</sup> · g <sup>-1</sup> )	Particle size (nm)	$I_{\max}$ (mV)	$I_{40\text{ns}}$ (mV)	$I_{40\text{ns}}/I_{\max}$ (%)	$\tau_{1/2}$ (ns)	$2\tau_{1/2}$ (ns)	$3\tau_{1/2}$ (ns)
Anatase A1	300	181	12	11.2	4.6	41	34	80	700
Anatase A2	600	42	27	5.0	2.2	44	28	3800	>10000
Anatase A3	800	13	63	6.8	4.8	71	800	>10000	
Anatase A4	850	9	65	7.8	5.8	74	800	>10000	
Anatase A5	900	9	67	9.6	7.2	75	1200	>10000	
Anatase B1	150	337	7.2	1.1	0.4	36	15	50	>200
Anatase B2	300	104	12.0	7.1	4.2	59	50	>200	
Anatase B3	600	39	26.6	8.6	6.8	79	>200		

concentration of hole traps in anatase and not in rutile. These traps are probably localized at the surface of the sample. The study of the influence of surface treatments will help to evidence it (cf. Section 4.4).

In the case of the rutile sample, an alternative explanation would be a fast trapping of electrons but this hypothesis will be kept out with experiments varying the laser intensity and with the study of the influence of water and ethanol at the surface.

#### 4.3. Influence of the laser intensity on the TRMC signal

The Fig. 5 displays  $I_{\max}$  and  $I_{40\text{ns}}$  versus laser intensity for 355 nm excitation for two representative rutile (R2) and anatase (B3) samples. The evolution of  $I_{\max}$

as a function of the laser intensity allows an elementary analysis of the phenomena during the excitation, i.e., the first 10 ns after the start of the pulse under the present experimental conditions.

For all samples, the curves  $I_{\max} = f(E)$  show the same behavior. At low intensities a linear relation is observed. With higher intensities, a sub-linear behavior appears, looking like a saturation phenomenon.

The number of charge-carriers created is linearly related to light intensity, it means to the number of incident photons. Therefore, if no excess charge carrier loss occurs during the excitation,  $I_{\max}$  should be linearly related to the laser intensity. The same relation is observed if one kind of charge-carriers is trapped during the excitation and no saturation of traps occurs (in other words if trapping is characterized by a single exponential

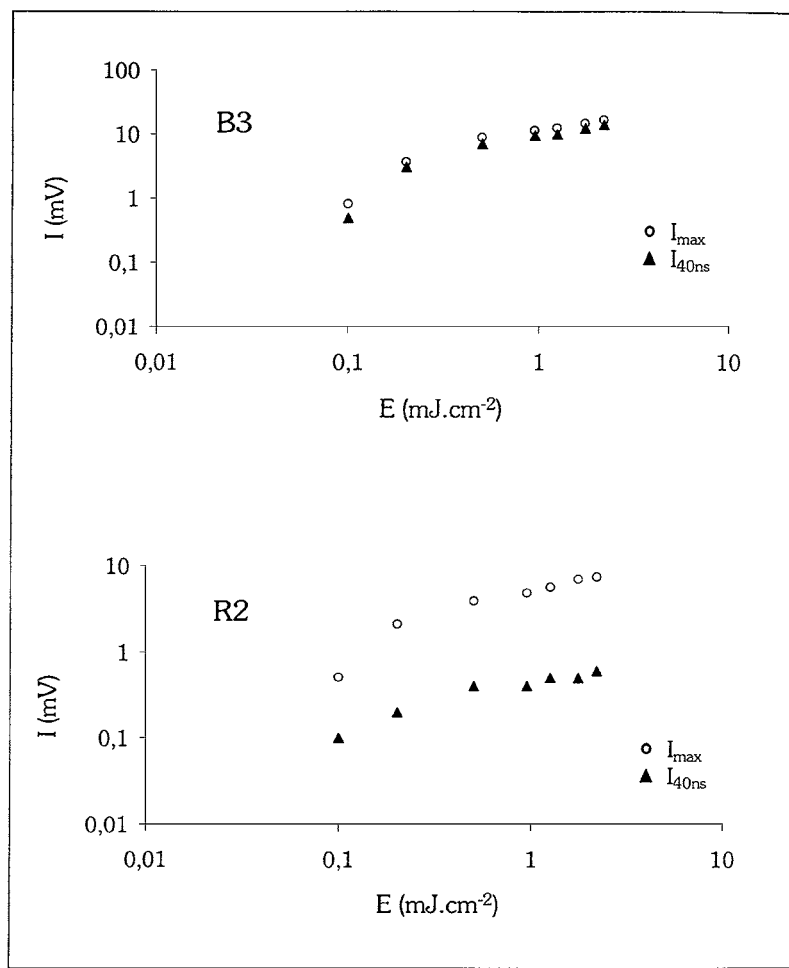


Figure 5 Influence of the laser intensity on the TRMC signal.

decay). On the other hand, if a phenomenon involving the two charge-carriers, like recombination, occurs during the pulse, this relation becomes sub-linear. It means that some charge-carriers disappear before 10 ns and the  $I_{\max}$  value is lowered. Thus, for all the samples, the  $I_{\max}$  saturation evidences fast recombination phenomena (already during the excitation pulse) at higher excitation densities.

In the case of anatase, the transition between the linear and the sub-linear dependence occurs at  $0.5 \text{ mJ} \cdot \text{cm}^{-2}$ . This is most easily explained by the presence of a fast electron-hole recombination that leads at high excess charge concentration (i.e., induced by a laser energy density exceeding  $0.5 \text{ mJ} \cdot \text{cm}^{-2}$ ) to appreciable excess charge-carrier decay by recombination during the excitation. Concerning rutile, this transition is observed at approximately the same energy density with the same explanation. However, the difference between both modifications is clearly observable on the  $I_{40 \text{ ns}}$  values. The signal on rutile at 40 ns is very small whereas an appreciable signal is detected at 40 ns for anatase (Fig. 5).

The fact that, for both modifications, the recombination is already active during the excitation indicates a very large recombination rate. In fact so large, that it implies a very fast TRMC decay between 10 ns and 40 ns, as it is observed for rutile. The behavior of anatase samples in the 10–40 ns range can only be explained if a quenching of this recombination occurs. The experiments described in the previous sections suggest that the most plausible candidate for this quenching process is the trapping of excess holes at the surface.

For 266 nm excitation, the number of experimental data does not suffice to analyze the behavior of  $I_{\max}$  as a function of the excitation density but, also in this case,

a linear dependence at low excitation density gives way to a sub-linear dependence at high excitation density.

#### 4.4. Influence of alcohol and water at the surface

On a powder sample, the ratio surface/volume is very high. Furthermore, crystalline defects, impurities and adsorbed species are preferentially localized on the surface. These are playing an important role in charge-carrier evolutions. They can act as trapping centers for one or both charge-carriers and so can accelerate the recombination. In order to understand the influence of the surface on charge-carrier lifetimes, experiments showing the effect of water and ethanol adsorbed on the surface have been realized.

The samples have been submerged in the considered liquid and a part of the centrifuged non-dried powder has been placed on the sample-holder. This treatment leads to a very slightly impregnated powder. It has been formerly verified that the solvents present no TRMC response. The observed TRMC signal really corresponds to charge-carriers created in the powder. The level of the TRMC response is comparable to non-treated powders and implies that the solvent do not absorb incident photons.

TRMC experiments carried out on rutile powders show no detectable effect due to the treatment.

The Fig. 6 shows the effect of water and ethanol on the TRMC signal of an anatase powder sample (B3).  $I_{\max}$  values have been normalized. This simple surface treatment modifies considerably the decay of the signal. This behavior shows the importance of surface phenomena and proves that some of the processes determining the decay, like hole trapping, occurs at the surface. This

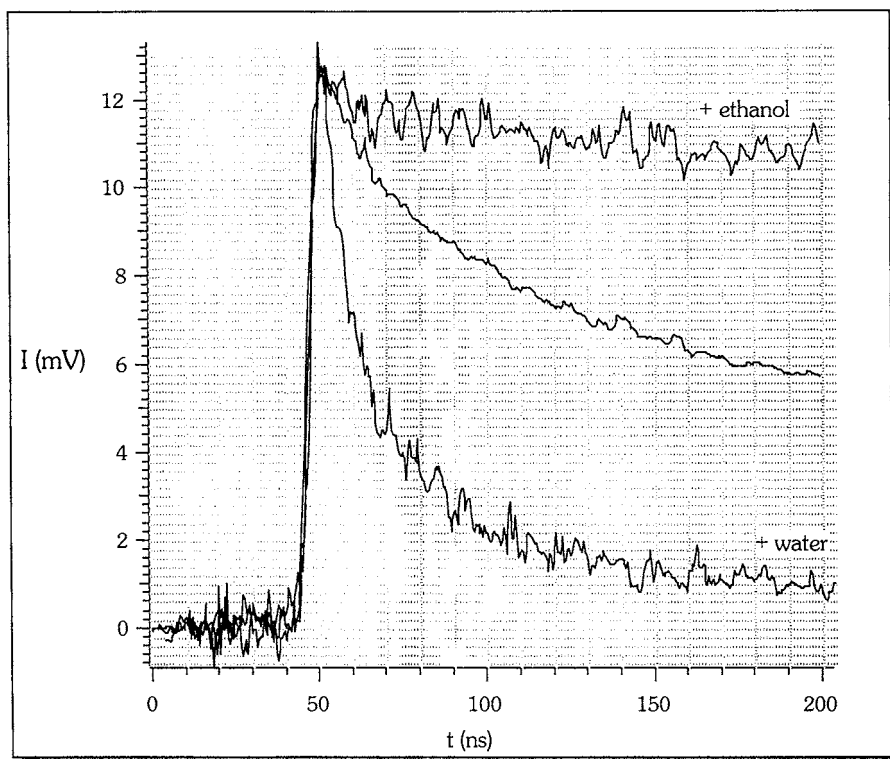


Figure 6 Effect of water and ethanol on the TRMC signal of anatase.

trapping has been explained as coming from a reaction between holes and surface hydroxyl groups ( $\text{OH}^-$ ) to form  $\text{OH}^\cdot$  radicals [18].

The Fig. 6 shows that the treatment with ethanol leads to a slower decay. This means a stabilization of the radicals and possibly an increase of the density of hole traps. This decreases the speed of hole relaxation in the valence band and slow down the recombination.

On the other hand, the water treatment leads to a faster decay. The water can either decrease the stability of radicals or act as electron scavenger reducing in that way their lifetime.

After few hours, the powder seems to be dried by evaporation. The signal of the ethanol-treated sample stays modified, whereas in the water-treated sample the initial signal is recovered. This indicates that a non-negligible quantity of alcohol remains adsorbed. The initial signal of the ethanol-treated sample is recovered by heating slightly the powder ( $70^\circ\text{C}$ ).

The fact that the rutile does not show any change after surface treatment allows thinking that there are not enough  $\text{OH}^-$  surface groups acting as hole traps. This point confirms the previous results showing that the fast decay in rutile is linked to recombination processes and not to surface trapping.

These treatments evidence the importance of surface phenomena and especially the role of hydroxyl groups. It was then interesting to find a surface treatment leading to a stable and permanent modification of the surface in order to control the carrier lifetimes.

Powders have been treated with highly acidic or basic solutions in order to clean up the surface but no radical and permanent change of TRMC signal has been observed on these samples. This would indicate that adding slightly  $\text{OH}$  groups on the surface does not change charge-carrier dynamics.

The literature describes more specific chemical ways to control the carrier lifetimes. It can be realized by surface modification by attachment of a sensitizer molecule to extend the photoresponse of the semiconductor [29]. At this time, TRMC studies on this kind of samples are on the run.

#### 4.5. Rutile

The fast decay observed in rutile powders (Fig. 4) makes characterization by considering the decay rather difficult. Most information is obtained from  $I_{\text{max}}$ , representing the electron mobility and the decay during the excitation, and the ratio between  $I_{40\text{ns}}$  and  $I_{\text{max}}$  representing the decay between 10 ns and 40 ns without imposing an exponential decay.

As general previous remarks, it is possible to mention that the larger part of the more than 25 rutile samples investigated are characterized by values of the  $I_{40\text{ns}}/I_{\text{max}}$  ratio smaller than 10%. This implies a very fast decay between 10 ns and 40 ns mainly determined by the shape of the excitation pulse. Furthermore, even for samples with an appreciable signal at 40 ns, a fast decay of the remaining signal is observed. Exceptions are samples containing more than a few percent anatase. For samples with 8% and 10% of anatase a value for  $I_{40\text{ns}}/I_{\text{max}}$  of about 25% was determined, where the re-

maining signal decay is characterized by a decay time largely exceeding 100 ns. More or less identically produced samples with lower anatase content show a low value for  $I_{40\text{ns}}/I_{\text{max}}$  ( $<10\%$ ) and a fast decay of the remaining signal.

For the rutile samples investigated, the signal amplitude  $I_{\text{max}}$  covers a range of about a factor of three.

In Table I, TRMC results of some exemplary rutile samples with different doping concentrations are displayed. As the differences in  $I_{\text{max}}$  are not very large and difficult to interpret, only the decay behavior will be discussed. It is clear that the decay rate increases with increasing Cr concentration, as it can be deduced from the decrease of the  $I_{40\text{ns}}/I_{\text{max}}$  ratio and the decrease of the decay time with Cr concentration. Also with increasing Nb concentration the decay rate increases.

The acceleration of the decay indicates a decrease of electrons lifetime by recombination or trapping. In the first assumption, the doping creates structural defects helping to recombination. The assumption of trapping can be explained as the following way: the substitution of  $\text{Cr}^{3+}$  by  $\text{Ti}^{4+}$  brings a negative charge. To keep electroneutrality,  $\text{TiO}_2$  must bring a positive charge, the addition of  $\text{Cr}^{3+}$  corresponds to p doping. As a general feature, the shift of the Fermi level linked to doping increases the number of trap-levels in the gap for the minority charge-carriers and decreases it for the majority carriers. In the case of Cr-doped  $\text{TiO}_2$ , it leads to the increase of holes lifetime and to the decrease of electrons lifetime by trapping.

In the case of  $\text{Nb}^{5+}$  doping (S1 and S2), the lifetime decreases also with the increase of the doping level. In this case, the doping is n type and according to the second assumption, this doping should lead to the increase of electrons lifetime and to the decrease of holes lifetime. The shift of the Fermi level by this kind of doping cannot be considered as a dominant effect. The decrease of the electrons lifetime should be linked to recombination assisted by the presence of levels in the gap, created by the insertion of foreign elements in  $\text{TiO}_2$  as Cr and Nb. These elements can be considered as impurities, and whatever their nature is, they favor recombination by creation of structural defects.

Interesting is the observation that coating of rutile powders by the oxides of Ce, Tb and Bi leads to very small values of  $I_{\text{max}}$ . It is tempting to attribute this phenomenon to the decrease of the light absorbed in the rutile particles. This would make the treated powders particularly appropriate as paints. However, other explanations of these experiments are possible.

#### 4.6. Anatase

As mentioned previously, all anatase samples show very slow TRMC decays compare to rutile samples. This was explained by hole trapping (at the surface) increasing the electron lifetime. The decay kinetics is then controlled at least partially by the relaxation rate of the trapped holes.

Also for anatase samples, some general trends can be noted. For about 20 samples produced in widely different ways, the ratio  $I_{40\text{ns}}/I_{\text{max}}$  is always larger than

25% and varies for the majority of the samples between 50% and 100%. This implies that, for the decay between 10 ns and 40 ns, the shape of the excitation pulse does not play an important role and this decay offers a very sensitive characterization of the sample. The values monitored for  $I_{\max}$  lie in the same range as found for rutile covering also approximately a factor of three.

TRMC results and structural properties of some anatase samples (A1 to B3) are collected in Table II. Samples from A set have been synthesized by the classical sulfate process while sample from B set have been synthesized by sol-gel route. From A1 to A5 and from B1 to B3, the only difference between sample preparations lies in the last thermal treatment (TT). X-ray diffraction shows that all the samples are 100% anatase phase.

It is impossible to compare directly samples of A and B series because they differ by their synthesis method, so the nature and level of impurity is not equivalent. Anyway, both series follow comparable behavior.

The results of Table II show that for both series, the decay rate decreases with increasing of TT temperature. Not only the decay rate between 10 ns and 40 ns but also the decay rate after 40 ns increase monotonously with the TT temperature. In the A series, the large value of  $I_{\max}$  for the A1 sample (TT at 300°C) is remarkable because the samples A2 to A4 suggest an increase of  $I_{\max}$  with the TT temperature. Obviously, different effects of TT influence  $I_{\max}$ . For the second (B) series,  $I_{\max}$  increases monotonously with the TT temperature. The crystalline quality, which depends on the number of impurities, defects or amorphous domains, results of the synthesis method and reagents. Unlike the impurities, the defects and amorphous domain can be controlled by TT. Anatase powders are synthesized by soft chemical routes in order to obtain nanosized particles, this leads to samples with high number of defects and amorphous domains. TT increases the size particle but minimizes their number. In any case for the B series, the increase of  $I_{\max}$  with the TT temperature shows the improvement of the crystallinity with TT.

An additional explanation of the fast decay of low temperature treated powders can be drawn. Around 10 nm particle sizes (A1 and B1 anatase), quantum size effects alter the internal electric field gradients and reduce the separation of electron-hole pairs. These effects should lead to high recombination rate.

The increase of the lifetime between 10 ns and 40 ns (from the increase of the  $I_{40\text{ns}}/I_{\max}$  ratio) with the TT temperature shows that TT increases the density of surface traps for holes. Furthermore, the stability of the trapped holes increases by TT as it can be concluded from the decrease of the TRMC decay rate after 40 ns with TT.

## 5. TRMC signal and photocatalytic activity

The measurements made on TiO<sub>2</sub> powders show the relevance of the TRMC method as analyses tool. We saw that the variation of parameters like structure, doping, synthesis process leads to significant variations of the TRMC signal.

However, the method suffers of some limitations in the case of rutile powders. This structural form shows a very fast TRMC decay. The signal has almost disappeared after 40 ns. Thus, phenomena like doping, which accelerate the decay, contribute to increase the lost of charge-carriers during the pulse. It decreases the  $I_{\max}$  value and results in a hardly detectable signal.

The experimental evidence presented in Section 4 indicates that absorption of UV light in rutile powders leads to the excitation of electrons and holes that disappear very quickly by recombination. Consequently, illumination leads mainly to the conversion of light in heat and probably in lesser extent in light (by luminescence). The probability of light induced surface reactions and so photocatalysis is small. On the other hand, it may be very stable as a white paint. The present experimental results suggest that the best stability against light will be observed for rutile powders with the smallest remaining signal at 40 ns. However, this suggestion must be considered as tentative because the transition between transient kinetics (as observed by TRMC measurements) and stationary kinetics (appropriate for the stability of paints) is by no means trivial. Besides, more information on the processes responsible for the signal amplitude at 40 ns and so the quenching of the recombination has to be available.

Furthermore, it has been showed that doping creates small but significant variations of the TRMC signal, anyway it was not possible to evidence some effect linked to the nature of the doping (p or n). The doping element plays only the role of an undetermined impurity. Indeed, it is the rate of doping element that influences the signal. It appears anyway that a low variation of Cr rate leads to noticeable variation of the signal that is less sensitive to the Nb variation. Thus, if the Cr rate is not very well known, effects linked to Cr might hide the study of the influence on the signal by an other doping element.

If the use of TRMC method as an analysis tool can be limited in the case of rutile, it is however not the case for anatase for which has proved to be very well adapted.

The TRMC signal, in the case of TiO<sub>2</sub>, gives a direct measurement of lifetime of free electrons created in the conduction band by a laser pulse. The difficulty to interpret the TRMC signal lies in the fact that numerous phenomena are responsible of the decay kinetics of free electrons. The simplest ones are the electron-hole recombination and the trapping of one or the other species. So, even if isolated, the information obtained on electron lifetime does not allow choosing between recombination and trapping. The information given by the decay has been coupled with studies of TRMC signal as function of surface treatment and laser intensity. This does not give an unambiguous interpretation of the observed signals, but only hypothesis corresponding to the most probable and very simple phenomena. It would be necessary to couple TRMC measurements with complementary experiments like EPR in order to detect the existence of trapping levels or surface analysis techniques to evidence adsorbed species, especially OH<sup>-</sup> on anatase.

One aim of this work was the interpretation of the TRMC signal in term of photocatalysis. The question is to understand if TRMC can be use directly as characterizing tool for photocatalytic materials.

The relation between TRMC signal decay and photoactivity is neither obvious nor immediate. The photocatalytic activity is linked to the presence of trapped charge-carriers at the surface, with lifetime long enough to react with the species to be photodegraded.

In the absence of bulk-trapping phenomena, only bulk recombination plays a role. In this case, a long TRMC signal would correspond to a slow recombination, so to high chargecarrier lifetimes that have enough time to migrate to the surface, it means good photoactivity. The relation becomes more complicated if bulk trapping also plays a role. One must add that in the case of titanium dioxide, an electrons bulk-trapping would correspond to an increase of the decay rate and a holes bulk-trapping to a decrease. It is, for this reason, difficult to draw the direct relation between a long TRMC signal and a high photocatalytic activity. In the light of the results of this work, in the case of TiO<sub>2</sub>, this relation might be made, because neither in rutile nor in anatase is observed a fast surface electron-trapping or a bulk hole-trapping.

However, the long TRMC decay in anatase powders shows the availability of electrons for catalytic reactions, whereas the excess holes are trapped at the surface. This relation between a long TRMC decay and a high photoactivity explains why anatase is the most favorable structural modification of TiO<sub>2</sub> for photocatalysis.

Experiments on TiO<sub>2</sub> powders on phenol photodegradation in water are now on the run in order to verify the hypothesis made before and to understand better the relation between structure, charge-carriers lifetimes and photoactivity.

## Acknowledgements

The authors thank Rhodia for the synthesis of the powders and for the financial support of this work.

It is also a pleasure to thank Professor Dr. H. Tributsch for fruitful discussions and Dr. G. Wallez for critically reading the manuscript.

## References

1. J. H. BRAUN, A. BAIDINS and R. E. MARGANSKI, *Progress in Organic Coating* **20** (1992) 105.
2. A. FUJISHIMA and K. HONDA, *Nature* **238** (1972) 37.
3. R. W. MATTHEWS, *Journal of Catalysis* **111** (1988) 264.
4. C. S. TURCHI and D. F. OLLIS, *ibid.* **122** (1990) 178.
5. A. WOLD, *Chemistry of Materials* **5** (1993) 280.
6. E. PELIZZETTI and C. MINERO, *Electrochimica Acta* **38**(1) (1993) 47.
7. A. SCLAFANI, L. PALMISANO and E. DAVI, *New Journal of Chemistry* **14** (1990) 265.
8. D. Z. WANG, *Appl. Catal. B: Envir.* **17**(3) (1998) 7.
9. H. TRIBUTSCH, private communication (1998).
10. R. F. HOWE, *Dev. Chem. Eng. Mineral Process* **6**(1/2) (1998) 55.
11. N. SERPONE, A. SALINARO, A. EMELINE and V. RYABCHUK, *J. Photochem. Photobiol. A: Chem.* **130** (2000) 83.
12. V. N. PARMON, *Catal. Today* **39** (1997) 137.
13. P. PICHAT, *J. Physique IV: Proceedings* **11** (2001) 141.
14. D. W. BAHNEMANN, *Res. Chem. Intermed.* **26**(2) (2000) 207.
15. S. MALATO, J. BLANCO, A. VIDAL and C. RICHTER, *Appl. Catal. B: Envir.* **37** (2002) 1.
16. J. M. WARMAN, M. P. DE HAAS, P. PICHAT, T. P. M. KOSTER, E. A. VAN DER ZOUWEN-ASSINK, A. MACKOR and R. COOPER, *Radiat. Phys. Chem.* **37**(3) (1991) 433.
17. K. M. SCHINDLER, M. BIRKHOLZ and M. KUNST, *Chem. Phys. Letters* **173**(5/6) (1990) 513.
18. K. M. SCHINDLER and M. KUNST, *ibid.* **172**(2) (1990) 137.
19. S. T. MARTIN, H. HERRMANN, W. CHOI and M. R. HOFFMANN, *J. Chem. Soc. Faraday Trans.* **90**(21) (1994) 3315.
20. S. T. MARTIN, H. HERRMANN and M. R. HOFFMANN, *ibid.* **90**(21) (1994) 3323.
21. J. M. WARMAN, M. P. DE HAAS, P. PICHAT and N. SERPONE, *J. Phys. Chem.* **95** (1991) 8858.
22. D. W. BAHNEMANN, M. HILGENDORFF and R. MEMMING, *ibid.* **B 101** (1997) 4265.
23. M. EDGE, R. JANES, J. ROBINSON, N. ALLEN, F. THOMPSON and J. WARMAN, *J. of Photochem. and Photobiol. A: Chem.* **113** (1998) 171.
24. K. M. SCHINDLER and M. KUNST, *J. Phys. Chem.* **94**(21) (1990) 8223.
25. M. KUNST and G. BECK, *J. Appl. Phys.* **60**(10) (1986) 3558.
26. *Idem.*, *ibid.* **63**(4) (1988) 1093.
27. J. M. WARMAN and M. P. DE HAAS, "Puls Radiolysis", Chap. 6 (CRC Press, 1991) p. 101.
28. S. J. FONASH, "Solar Cell Device Physics" (Academic Press, New York, London, 1981).
29. P. V. KAMAT, *Chem. Rev.* **93** (1993) 267.

Received 10 June 2002

and accepted 21 January 2003